THE JOURNAL OF PHYSICAL CHEMISTRY B

Article

pubs.acs.org/JPCB

Effects of Concentration on Like-Charge Pairing of Guanidinium Ions and on the Structure of Water: An All-Atom Molecular Dynamics Simulation Study

Dibyendu Bandyopadhyay,[†] K. Bhanja,[†] Sadhana Mohan,[†] Swapan K. Ghosh,[‡] and Niharendu Choudhury*[,‡]

[†]Heavy Water Division and [‡]Theoretical Chemistry Section, Bhabha Atomic Research Centre, Mumbai 400 085, India

Supporting Information

ABSTRACT: Like-charge ion-pair formation in an aqueous solution of guanidinium chloride (GdmCl) has two important facets. On one hand, it describes the role of the arginine (ARG) side chain in aggregation and dimer formation in proteins, and on the other hand, it lends support for the direct mechanism of protein denaturation by GdmCl. We employ all-atom molecular dynamics simulations to investigate the effect of GdmCl concentration on the like-charge ion-pair formation of guanidinium ions (Gdm^+). From analyses of the radial distribution function (RDF) between the carbon atoms of two guanidinium moieties, the existence of both contact pairs and solvent-separated pairs has been observed. Although the peak height corresponding to the contact-pair state decreases, the number of Gdm^+ ions in the contact-pair state actually increases with increasing GdmCl concentration. We have also investigated the effect of the concentration of Gdm^+ on the structure of water. The effect of GdmCl concentration on the radial and tetrahedral structures of water is found to be negligibly small; however, GdmCl concentration has a considerable effect on the hydrogen-bonding structure of water. It is demonstrated that the presence of chloride ions, not Gdm^+, in the first solvation shell of water causes the distortion in the hydrogen-bonding network of water. In order to establish that Gdm^+ not only stacks against another Gdm^+ but also directly attacks the ARG residue of a protein or peptide, simulation of an ARG-rich peptide in 6 M aqueous solution of GdmCl has been performed. The analyses of RDFs and orientation distributions reveal that the Gdm^+ moiety of the GdmCl attacks the same moiety in the ARG side chain with a parallel stacking orientation.

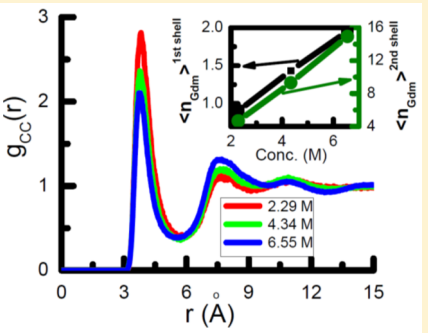

1. INTRODUCTION

Guanidinium chloride (GdmCl) and urea at high concentrations (≥5 M) are popular denaturants[1−13] of proteins and nucleic acids. Of these two denaturants, the guanidinium ion (Gdm^+) of GdmCl is a positively charged ionic species; therefore, it is expected to act in a different manner than urea. The Gdm moiety structurally resembles a part of the arginine (ARG) side chain of the protein. The clustering of ARG residues in many proteins indicates that the ARG−ARG interaction at protein interfaces stabilizes the protein−protein interaction,[14−20] and the Gdm−Gdm interaction inside the core is one of the driving forces for protein folding and stability. However, the Gdm moiety being positively charged, stacking of two such moieties is counterintuitive. In fact, like-charge ion−ion interactions in condensed phases are prevalent, and their different manifestations are intriguing and important in view of their relevance in the chemical, biological, and physical sciences. It is well known from Coulomb's law that like-charge ions repel each other. However, in condensed phases, because of the presence of many other species, like-charge ion-pair formation is possible. In this context, formation of an ion-pair between two Gdm^+ ions in an aqueous solution of GdmCl[21−26] is of special interest for several reasons. First, GdmCl acts as an effective denaturant for proteins and nucleic acids, and therefore it is essential to know the mechanism of its action and its relationship with the ion-pair formation. Apart from that, the structural similarity of Gdm^+ with the ARG side chain of a protein may explain the conglomeration[14−20] of multiple ARG residues in many proteins. Moreover, the guanidinium−water system is a simple and important test case for understanding the origin of like-charge attraction in condensed phases.

Despite many theoretical and experimental studies[27−54] over the years, the molecular mechanism by which Gdm^+ acts as a denaturant for proteins and nucleic acids in aqueous solutions remains unresolved. Many early studies[29,30] indicated alterations in hydrophobic interactions[55,56] as a cause for the denaturation. Many groups[40−53] pointed out that the denaturation by GdmCl is effected by preferential solvation of nonpolar groups of the macromolecules. However, opinions are divided on whether it is a direct or an indirect mechanism that dictates the denaturation process. The indirect mechanism[27−44] posits that the denaturant

Special Issue: Biman Bagchi Festschrift

Received: March 31, 2015
Revised: June 16, 2015

DOI: 10.1021/acs.jpcb.5b03064
J. Phys. Chem. B XXXX, XXX, XXX−XXX

first breaks the tetrahedral and hydrogen-bonded network of water and thereby helps water indirectly to invade the interior of a protein or nucleic acid. On the other hand, the direct mechanism[45−54] predicts that Gdm^+ first attacks polar as well as nonpolar residues of the protein and causes the macromolecule structure to open up.

With regard to the direct mechanism, it is important to know how two ARG groups in proteins behave. As already mentioned, the existence of conglomeration of ARG groups in many proteins has direct relevance to protein folding and to the stability of protein−protein interactions. Many ARG-based synthetic drug molecules have been synthesized, based on this ARG−ARG pair formation propensity. Gdm^+ can interact with a protein moiety through a direct Coulomb interaction or through a van der Waals interaction. However, conglomeration of ARG or ion-pairing of Gdm^+ ions in aqueous solution is counterintuitive as two same-charge ions come close to each other, which signifies the role of the van der Waals or dispersion interaction. It is now almost certain that Gdm^+ ions at high concentrations form like-charge ion-pairs in solution.

In an early study using neutron diffraction experiments, Mason et al.[57] showed that Gdm^+ in its aqueous solution is one of the most weakly hydrated cations, and they posited that, due to this weak hydration, denaturation takes place via a direct preferential mechanism. However, subsequent neutron scattering and molecular dynamics (MD) simulation study by Brady and co-workers[58] showed that Gdm^+ has a well-defined hydration shell. The bimodal hydration structure of Gdm^+ with the N−H groups makes well-ordered hydrogen bonds (HBs), whereas it has been predicted that the planar face is relatively deficient in interaction with water. The most important outcome of this study was the identification of like-charge ion-pairing of Gdm^+ ions which are stacked parallel to each other. The researchers justified that this parallel stacking ability enables Gdm^+ to interact favorably with the hydrophobic, aromatic side chains of the protein.

A recent computational study by Vazdar et al.[24] using ab initio MD simulation also identified like-charge ion-pairing. Amphiphilic character and van der Waals interaction between the Gdm^+ ions have been postulated to be responsible for such contact ion-pair formation defying like-charge repulsion. Jungwirth and co-workers[26] used MD simulation and capillary electrophoresis experiments to demonstrate that guanidinium cations form like-charge ion-pairs with the positively charged side chains of ARG-containing peptides in aqueous solutions, but they found no such effect for sodium cations and/or lysine polypeptide. The orientational dependence of the affinity of the Gdm^+ ions at the water−vapor interface was also investigated, and it was found that the population of Gdm^+ ions oriented parallel to the interface is greater at the surface region than in the bulk. For other orientations, the trend is the opposite.[27] In fact, like-charge ion-pair formation in aqueous solution of GdmCl was predicted[21,23] by calculating the potential of mean force (PMF) between two Gdm^+ ions in water. Although a contact-pair minimum has been observed, the stability of the contact-pair state was shown[23] to be dependent on the details of the model. Most of these studies used either infinitely dilute solution or a solution with a finite concentration of Gdm^+.

Although many recent studies on protein denaturation by GdmCl have argued in favor of a direct mechanism, it is also worthwhile to know whether Gdm^+ breaks the tetrahedral and hydrogen-bonding network of water. Gdm^+ is known to be an effective denaturant for proteins and nucleic acids when present at high concentration in its aqueous solution. Therefore, knowing the effect of GdmCl concentration on the formation of Gdm^+ ion-pairs and on the tetrahedral and hydrogen-bonding structures of water is essential. In fact, a recent MD simulation study[51] of aqueous solutions of GdmCl at different concentrations addressed this issue, finding like-charge ion-pairing at moderate GdmCl concentrations, but contrary to the general intuition that an increase in GdmCl concentration would increase ion-pair formation, those results predicted a decrease in the population of contact-pair states and a subsequent increase in solvent-separated states. However, this conclusion was based on a comparison of the first and second peaks of the Gdm−Gdm radial distribution function (RDF), $g_{CC}(r)$, at different concentrations. At this point, it is important to mention that a simple comparison of the peak heights of Gdm−Gdm RDFs of solutions with unequal concentrations is erroneous, as the individual RDF is normalized by the respective bulk concentration. Mandal et al.[51] also showed that both the tetrahedral and hydrogen-bonding structures of water are broken with increasing concentration of GdmCl. In calculating these quantities, they considered only water (not any sites of Gdm^+ and chloride ion, Cl^-) as neighbors. However, in a concentrated solution of Gdm^+, which has many potential hydrogen-bonding sites, it is expected that some of the first solvation shell "water neighbors" will be replaced by Gdm^+ and/or Cl^-. In fact, we have shown recently[59,60] in the case of aqueous urea solution that, in a sufficiently concentrated urea solution, the probability of the fourth neighbor (distance-wise) being a urea molecule is about 37% in a 9 M urea solution. It is shown that normal calculation of the tetrahedral order parameter by considering the four nearest "water neighbors" around a water molecule leads to an erroneous result, as the probability of the fourth "water neighbor" being outside the solvation shell increases at high concentrations. Thus, proper choice of nearest neighbors is essential in such cases. It is therefore important to revisit the MD results on GdmCl aqueous solution and check whether really like-charge ion-pair formation decreases with increasing GdmCl concentration and whether GdmCl really breaks the water structure.

In this work, we have performed MD simulations of aqueous solutions of GdmCl at varying concentrations to verify the effect of increasing concentration of GdmCl on the like-charge ion-pair formation as well as on the local structure of water. In order to investigate the direct interaction mechanism aspect of chemical denaturation of a protein by GdmCl, we have also simulated an ARG-rich peptide in an aqueous solution of 6 M GdmCl. In this case, it is important to know whether Gdm^+ of the GdmCl salt attacks the Gdm moiety of the ARG side chain and, if so, whether they form a parallel stacking orientation. It is also important to know which part of the ARG side chain of the protein/peptide is directly attacked by Gdm^+ of GdmCl. In what follows, in section 2 are discussed the models used and the simulation methods adopted. In section 3.1, the results on the dependence of GdmCl concentration on like-charge ion-pair formation are discussed. In section 3.3, the effects of increasing concentration of GdmCl on the radial, hydrogen-bonding, and tetrahedral structures of water are discussed. In section 3.4, the results on dynamic properties of different species in solution at various GdmCl concentrations are presented. In section 3.5, we discuss the results obtained from a simulation of an ARG-rich peptide in 6 M aqueous GdmCl solution. Finally, concluding remarks summarizing the main outcome of this work are presented in section 4.

DOI: 10.1021/acs.jpcb.5b03064
J. Phys. Chem. B XXXX, XXX, XXX−XXX

2. MODELS AND METHODS

The force field used for Gdm^+ is fully flexible with bond, angle and dihedral terms in the intramolecular potential along with usual nonbonded Lennard-Jones and Coulomb interactions. Namely CHARMM22 force field[51,58] has been used for Gdm^+. For water, we use the TIP4P/2005[61] rigid-body atomistic model with fixed bond lengths and bond angles. This new variant of the TIP4P model is superior to the original TIP4P model in terms of reproducing most of the anomalies of water. However, in order to reproduce the results obtained by Mandal et al.,[51] we have also used the TIP3P water model. Some of our results with the TIP3P model are shown in the Supporting Information. Different concentrations of aqueous solutions of GdmCl are prepared by randomly placing requisite number of GdmCl molecules in a pre-equilibrated water box of appropriate size. Specific details of the numbers of GdmCl (N_{GdmCl}) and water (N_W) molecules and GdmCl mole fraction (X_{GdmCl}) with the volume of the boxes and molarity of the resulting solutions are given in Table 1.

Table 1. Different Systems Simulated in This Work

system	N_{GdmCl}[a]	N_W[a]	X_{GdmCl}[a]	volume (nm^3)	molarity (M)
1G	0	512	0.0	15.365	0.0
2G	42	870	0.04605	30.469	2.289
3G	84	768	0.09859	32.157	4.338
4G-1	125	587	0.1755	31.704	6.548
4G-2	500	2350	0.1754	126.582	6.558

[a] N_{GdmCl} and N_W are the numbers of GdmCl and water molecules, respectively, and X_{GdmCl} is the GdmCl mole fraction.

In order to prepare the peptide−water−GdmCl system, an ARG-rich 26-residue peptide (PDB ID: 2MIA)[62] was immersed into a pre-equilibrated solution of 6 M GdmCl. All the overlapping water molecules were removed. The final starting configuration thus has one peptide molecule immersed in a cubic simulation box (with box size around 6.7 nm) containing 6000 water and 1100 GdmCl molecules. A snapshot of the simulation system is shown in Figure 1A. Out of the 26 residues of the peptide, 11 residues of 2MIA peptide are ARG residues. This side chain of the ARG is shown in Figure 1B.

All the simulations were performed using GROMACS[63] simulation package. After initial energy minimization, all the simulations were run in the NPT ensemble,[64] with periodic boundary conditions, using the MD extended system approach[64] of Parrinello and Rahman[65] to fix pressure and the Berendsen algorithm[66] to fix temperature. For water, we constrained the bonds and the angle of a water molecule by the SHAKE algorithm,[67] and electrostatic interactions were calculated using particle-mesh Ewald method.[68,69] Equations of motions were integrated using Leap-frog algorith[64] with a time step of 0.5 fs. All the simulations were carried out at a target pressure of 1 atm and a target temperature of 300 K. For equilibration of the GdmCl solution, we discarded the first 20 ns of trajectories, and the trajectories for the next 10 ns were stored for analyses. In order to check the effect of finite box size and finite length of simulation trajectory, we also performed a simulation of ∼6 M GdmCl solution with a larger box. In this case, we had 500 GdmCl molecules and 2350 water molecules with a box size of 5.021 nm. In the case of smaller system sizes (systems 1G, 2G, 3G, and 4G-1; see Table 1), we discarded the first 20 ns of trajectories for equilibration, and the trajectories for the next 10 ns were stored for analyses. For the larger GdmCl−water system (system 4G-2), we discarded the first 60 ns of trajectories for equilibration, and the next 5 ns were used for further analyses. For the protein solution, we discarded the initial 50 ns of trajectories for equilibration, and the next 10 ns of trajectories were stored for analyses. Most of the post analyses of the simulation trajectory were performed using our in-house-written software. Only various RDFs involving protein residues were obtained from GROMACS analyses programs.

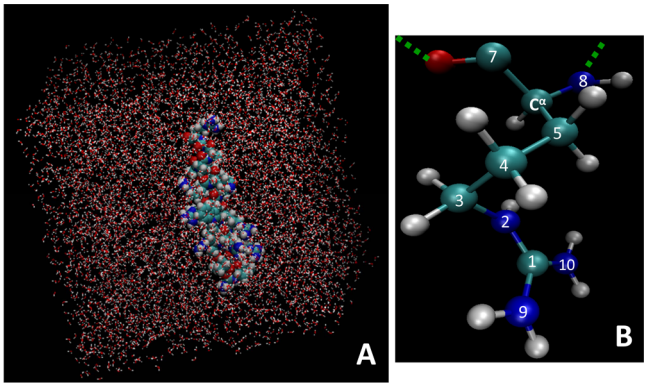

Figure 1. (A) Snapshot of a typical configuration of peptide−water system. (B) The arginine residue, shown as a ball-and-stick model. Blue atoms are nitrogen, red atoms are oxygen, green atoms are carbon, and gray atoms are hydrogen. Dashed lines show the extension of the main chain.

2.1. Local Orders. We know that, in the case of a perfectly tetrahedral structure, there are four nearest neighbors in the first solvation shell of a central molecule. Oxygen−oxygen RDF of water describes radial arrangements of neighboring water around a reference, central water molecule, but cannot provide any information about the angular preferences of the neighboring molecules. In order to get information about angular preferences of the neighbors around a central water molecule, an order parameter known as tetrahedral order parameter is used. In order to assess structural (hydrogen-bonding) integrity in the presence of solutes or salts, average number of HBs and the distribution of hydrogen-bonding angle will be useful used.

2.2. Tetrahedral Order Parameter. In this approach, a tetrahedral order parameter q_i is defined for each water molecule in the system by considering its four nearest neighbors. The parameter q_i is defined by[70]

$$q_i = 1 - \frac{3}{8}\sum_{j=1}^{3}\sum_{k=j+1}^{4}\left[\cos\theta_{jik} + \frac{1}{3}\right]^2 \quad (1)$$

where i is the central molecule and θ_{jik} is the angle formed by neighbors j and k at the reference, central water molecule i. For a perfect tetrahedral angle, $\cos\theta_{jik} = -1/3$ and thus $q_i = 1$ and for a perfectly random arrangement, angular integration of the term within square bracket in eq 1 yields 4/9. Since there are four neighbors and therefore six angles in the summation, this contribution come out to be 8/3. Therefore, the prefactor 3/8 before summation makes the second term 1 and hence $q_i = 0$ for a random arrangement.[70] The above equation is valid for a central molecule with four nearest neighbors. In the present investigation, we used the above equation for water molecules with two and three neighbors by modifying the constant term before the summation. Details of how these normalization constants were calculated are given by Bandyopadhyay et al.[60] The average value q_4, the tetrahedral order parameter, is

DOI: 10.1021/acs.jpcb.5b03064
J. Phys. Chem. B XXXX, XXX, XXX−XXX

calculated by averaging over all the N molecules and over the ensemble using the following equation,

$$q_4 = \frac{1}{N}\langle \sum_{i=1}^{N} q_i \rangle \quad (2)$$

2.3. Hydrogen Bond. Water is a network forming hydrogen-bonded liquid. Two important order parameters namely average number of hydrogen bonds ($\langle n_{HB} \rangle$) and its distribution are used to gauge any change in hydrogen-bonding structure of water. The standard geometric criterion, according to which two water molecules are considered to be hydrogen-bonded only if (i) the inter-oxygen distance is less than 3.5 Å, (ii) the hydrogen−oxygen (hydrogen-bonded) distance is less than 2.45 Å, and (iii) the H−O···O angle (often known as HB angle and denoted by θ_{HB}) is less than 30°, has been used to identify a HB between two water molecules.

3. RESULT AND DISCUSSION

3.1. Ion-Pair Formation and Its Concentration Dependence. Let us first discuss like-charge ion-pair formation of the Gdm^+ ions. The effect of Gdm^+ concentration on the extent of like-charge ion-pair formation can be estimated from the change in Gdm−Gdm RDF with concentration. In Figure 2, we

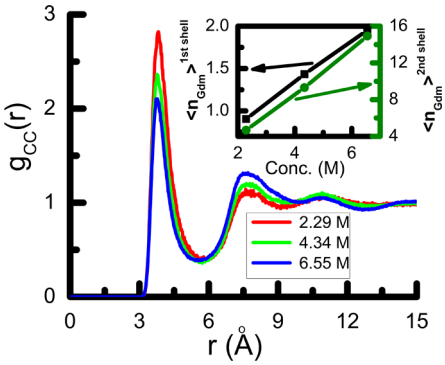

Figure 2. Radial distribution functions of the carbon atom of the guanidinium moiety around the same for three different concentrations. Distance r is measured as intermolecular distance between the carbon atoms of two Gdm moieties. In the inset, numbers of Gdm^+ ions in the first (shown by black line and left-hand-side axis) and second (shown by green line and right-hand-side axis) solvation shells have been shown.

therefore show the RDF among carbon atoms of the Gdm^+ ions, $g_{CC}(r)$, at different concentrations of the GdmCl. The large first peak at 3.7−3.8 Å between two carbon atoms signifies not only aggregation but also stacking (parallel orientation) of the like-charge Gdm^+ ions. Had it been in-plane side-by-side pairing, the carbon−carbon distance would have been more. In order to check whether there is any water molecule present between two Gdm^+ ions stacked parallel to each other, we plotted the RDF, $g_{C\text{-}Ow}$, between the carbon atom of the Gdm^+ and the oxygen atom of water (see lower panel of Figure 3). The first peak at around 3.7 Å between carbon atom of Gdm^+ and oxygen atom of water confirms that there is no water molecule between two Gdm^+ ions at their closest separation. If we look at the RDF of Cl^- around the carbon of Gdm^+ as shown in Figure 3 upper panel, it is clear that the first peak appears at around 4 Å. Therefore, Cl^- also does not come between two stacked Gdm^+ ions. The second peak of $g_{CC}(r)$ in Figure 2 is at around 7.7 Å and represents the solvent-separated state. Similar observations have

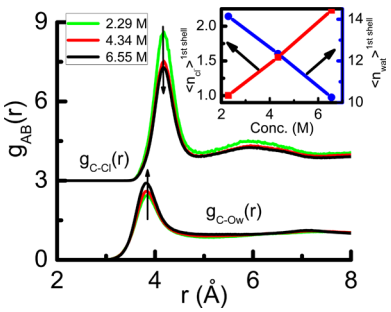

Figure 3. Radial distribution functions of O_w of water (lower panel) and chloride ion (upper panel) around the carbon atom of guanidinium moiety. The RDF of the chloride ion, $g_{C-Cl}(r)$ is shifted upward by 3 units for clarity. In the inset, numbers of chloride ions (shown by red line and left-hand axis) and water molecules (shown by blue line and right-hand axis) in the first solvation shell of the Gdm^+ ion are shown.

been made earlier.[51] Recently Vazder et al.[22,24] using ab initio MD simulation have also found existence of counterintuitive like-charge Gdm^+−Gdm^+ ion-pair formation. The stability of such "electrostatics-defying" ion-pairs in a stacked conformation has been attributed to the amphiphilic nature of Gdm^+. Due to planarity, aromaticity, and non-uniform charge distribution, the faces of the Gdm^+ cation are hydrophobic and weakly hydrated, whereas the Gdm^+ forms HBs with water molecules in its molecular plane.[22,24]

The most surprising observation is the way RDF changes with increasing GdmCl concentration. With increasing concentration of GdmCl, height of the first peak of the $g_{CC}(r)$ decreases and that of second (solvent-separated state) peak increases (see Figure 2). It is very tempting to conclude from these changes in RDF that Gdm^+−Gdm^+ contact-pair formation decreases and solvent-separated pair formation increases with increasing GdmCl concentration. Mandal et al.[51] have observed similar variation in RDF and inferred that extent of contact ion-pair state is decreasing with increasing GdmCl concentration and that of solvent-separated state is increasing. However, it is very important to note at this point that RDFs at different concentrations are normalized by respective bulk concentration and therefore comparing the peak heights of RDFs for estimating number of molecules in the solvation shells at two different concentrations is misleading. Although the height of the first peak of a RDF is a measure of density of contact-pair state relative to bulk concentration, it does not tell us about the absolute number of nearest neighbors. In this situation, it is better to integrate the RDF up to appropriate distances corresponding to the first and second solvation shells to get the number of Gdm^+ ions in contact-pair and solvent-separated states, respectively. To find whether formation of contact-pair states is really decreasing with increasing GdmCl concentration, we integrated the $g_{CC}(r)$ up to the first minimum of RDF. In the inset of Figure 2, we show the numbers of Gdm^+ moieties in the first and the second solvation shells as a function of GdmCl concentration. It is interesting to observe that numbers of Gdm^+ ions in both contact-pair state (black line, left-hand axis) and solvent-separated state (green line, right-hand axis) increase with increasing concentration. It is important to emphasize that contrary to the observation based on peak heights of the RDFs, actual number of ions present in the first and second shells follow monotonic increase with GdmCl concentration. However, maximum number molecules a solvation shell of a particular species can accommodate is restricted by molecular geometry

DOI: 10.1021/acs.jpcb.5b03064
J. Phys. Chem. B XXXX, XXX, XXX−XXX

and packing. Therefore, number of solvation shell molecules may not be linearly increased by further increase of GdmCl concentration. Thus, the result presented so far demonstrates that the formation of like-charge ion-pairs as well as solvent-separated ion-pairs does not really decrease with GdmCl concentration. Both are increasing with increasing GdmCl concentrations. As far as water and Cl^- are concerned (see Figure 3) the integrated value of the number of water molecules in the first solvation shell of Gdm^+ decreases and the number of Cl^- ions increases (see the inset of Figure 3). Thus, as the concentration of GdmCl increases, number of water molecules decreases and the number of Cl^- ions increases in the first solvation shell of a Gdm^+. The formation of ion-pair and its increase with increase in GdmCl concentration has a special significance in denaturation mechanism. The higher propensity of the Gdm^+ moiety to undergo like-charge ion-pair formation at high concentration implies that these Gdm^+ ions will form similar like-charge ion-pairs with the ARG and other similar aromatic moieties of the protein residues and thereby replace water molecules from the protein surface and denature it. Our observation here is based on the improved TIP4P/2005 water model. However, all the trends in the results are the same if we use the TIP3P water model as used earlier.[51] All the results using the TIP3P model of water are given in the Supporting Information. As already mentioned, in order to check the reliability of the results presented here with respect to system size and finite time dependence, we further simulated the highest concentration GdmCl solution by considering a larger system size and for a longer time (see system 4G-2 in Table 1). The calculated RDFs between two Gdm^+ carbon atoms, the carbon atom of the Gdm^+ and Cl^-, the carbon atom of Gdm^+ and oxygen of water, and between oxygen−oxygen (of water) are shown in Figure S5 of the Part B of the Supporting Information. Results from smaller system size and shorter simulation trajectories are compared with those obtained from larger box size and longer simulation time, and in all the cases excellent agreements have been observed indicating the results presented here based on smaller system size and shorter trajectories are trustworthy.

3.2. Stacking of Guanidinium Ion Moieties. The implications of the stacking of Gdm moieties at a reasonably high GdmCl concentration in its aqueous solution are two-fold. Close-stacking of guanidinium moieties indicates that this denaturant attacks the protein residues of similar nature and gets stacked into the protein interior and interfaces, thus denaturing the protein by a direct interaction mechanism. In order to get an idea about the relative orientation of the two Gdm^+ ions in solution in its contact-pair state, we calculated the distribution of the angle ϕ between two molecular planes of two Gdm moieties. The schematic representation of the two molecular planes inclined at an angle ϕ is shown in Figure 4. The distributions $P(\phi)$ of the angles ϕ made by the Gdm^+ moieties present in the contact-pair state for three different concentrations of GdmCl have been shown in Figure 5. Two peaks near 0° and 180° in the distribution signify almost parallel stacking orientation between two Gdm^+ moieties. As the concentration of GdmCl is increasing, there is a slight reduction in the peak heights (as in the case of $g(r)$, Figure 2). This slight decrease is due to variation in bulk concentrations.

On the other hand, the ARG residue of a protein resembles a guanidinium moiety. Despite the highly repulsive nature of closely spaced like-charged groups, close stacking of ARG residues in a protein structure has been often observed.[14−16] Thus, Gdm^+−Gdm^+ stacking may have direct relation with

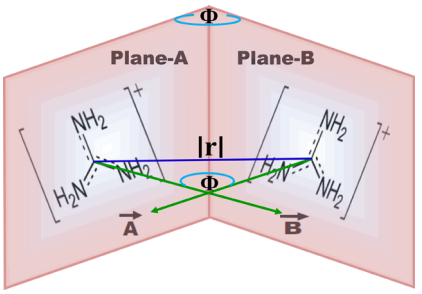

Figure 4. Schematic representation of two molecular planes of guanidinium ions inclined at an angle ϕ.

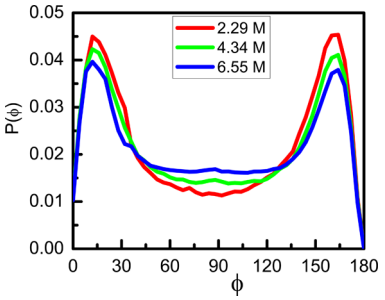

Figure 5. Distributions $P(\phi)$ of the angles ϕ made by the perpendiculars drawn from two guanidinium molecular planes at three different GdmCl concentrations.

protein folding and stability. Since denaturation of protein occurs at a high temperature, it is therefore expected that parallel stacking orientation between two ARG moieties will be disrupted at a high temperature. In order to check the effect of temperature on the parallel stacking orientation between two Gdm^+ ions, we simulated an aqueous solution of GdmCl at different temperatures and calculated the distribution of the angle ϕ; those results are shown in Figure 6. As expected, we found that at higher

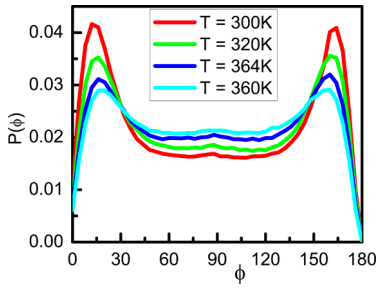

Figure 6. Distributions $P(\phi)$ of the angles ϕ made by the perpendiculars drawn from two guanidinium molecular planes at four different temperatures.

temperatures, preferred parallel orientation of the Gdm moieties gets disrupted and orientation becomes almost homogeneous. Thus, it indirectly supports the fact that, during high-temperature denaturation, close parallel stacking of ARG moieties gets disrupted with no preferential orientation.

It is well known that purely hydrophobic solutes aggregate in water and for nanoscopic or larger hydrophobic solutes, the spontaneous contact-pair formation is dewetting induced.[55,56] The analysis of PMF of nanoscopic hydrophobic solutes has demonstrated[55] a huge stabilizing (negative) solvent-induced contribution to the PMF at a distance corresponding to the contact-pair formation. In the present case, the PMF values

DOI: 10.1021/acs.jpcb.5b03064
J. Phys. Chem. B XXXX, XXX, XXX−XXX

$(w(r))$ between guanidinium moieties at different concentrations have been calculated from the $g(r)$ between two Gdm moieties as

$$w(r) = -k_B T \ln g_{CC}(r) \quad (3)$$

where k_B and T are Boltzmann constant and temperature in kelvin, respectively. The difference between total PMF and direct interaction, $U_{solu}(r)$, between the solutes gives rise to the solvent contribution, $w_{solv}(r)$ to the total $w(r)$, viz.,

$$w(r) = U_{solu}(r) + w_{solv}(r) \quad (4)$$

In order to get direct solute−solute interaction component, we performed vacuum (without any water molecule) simulation of GdmCl at different concentrations. The carbon−carbon (of Gdm moieties) RDF calculated from the vacuum simulation is then converted according to eq 3 to get $U_{solu}(r)$. Finally, solvent-induced contribution to PMF has been obtained by subtracting $U_{solu}(r)$ from $w(r)$ according to eq 4. These quantities are shown in Figure 7. It is interesting to observe that the first minimum of

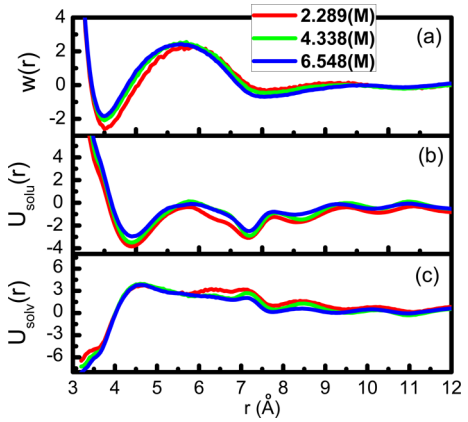

Figure 7. (a) Potential of mean force values $(w(r))$ among the guanidinium moieties at three different concentrations of GdmCl salts. (b) Direct solute−solute interaction $U_{solu}(r)$ as obtained from vacuum simulations of GdmCl at different concentrations. (c) Solvent-induced contribution, $w_{solv}(r)$, to the PMF at different GdmCl concentrations.

$U_{solu}(r)$ appears (see Figure 7b) at a larger distance than that of $w(r)$. Since in vacuum simulation there are no water molecules, two positively charged Gdm^+ moieties cannot come very close to each other. It therefore appears that the close stacking of Gdm^+ ions in the aqueous solution (see Figure 2 or 7a) is stabilized by the presence of the water molecules. The contribution of the solvent to this stabilization is demonstrated by solvent contribution $(w_{solv}(r))$ to the PMF. From the plots of $w_{solv}(r)$ as shown in Figure 7c, it is evident that the solvent induced contribution is stabilizing (negative) the contact-pair state. However, not so much dependence of the concentrations of the GdmCl was observed in the $w_{solv}(r)$.

It is important to note that Mandal et al.[51] misinterpreted the decrease in the peak height of the first peak of $g_{CC}(r)$ with GdmCl concentration as a decrease in the ion-pair formation. As denaturation occurs at sufficiently high GdmCl concentration, therefore they ruled out the direct interaction mechanism. They subsequently demonstrated that indirect mechanism by breaking the water structure is responsible for GdmCl's action as protein denaturant. In order to look into this aspect, in the following section we present results on the effect of GdmCl concentration on water structure.

3.3. Effect of Guanidinium Chloride Concentration on Water Structure. Although indirect evidence suggests that Gdm^+ denatures protein by direct preferential interaction, existence of the indirect mechanism, which posits breakdown of water structure as a reason for chemical denaturation, cannot be ruled out unless effect of GdmCl on the water structure is examined. Therefore, here we present the effect of increasing GdmCl concentration on the local structure of water. Water is a three-dimensional hydrogen-bonded network of tetrahedral structures. In order to assess the effect of GdmCl concentration on water structure, we therefore looked into details of radial, tetrahedral, and hydrogen-bonding structures of water.

3.3.1. Radial Structure. One usual way of looking at the radial structure of a fluid is by looking into the RDF. Although RDF gives average radial structure, detailed information about the radial structure can be obtained by following nearest neighbor approach.[59] In order to check whether the structure of water changes with increasing concentration of GdmCl, we therefore calculated the distribution of radial distances of the nearest neighbors. In the case of bulk water, we know that there are on average four water neighbors around a central water molecule. We show the distributions of the first four "water neighbors", $P(r_n^w)$, with $n = 1-4$, in Figure 8. It is seen that the distributions

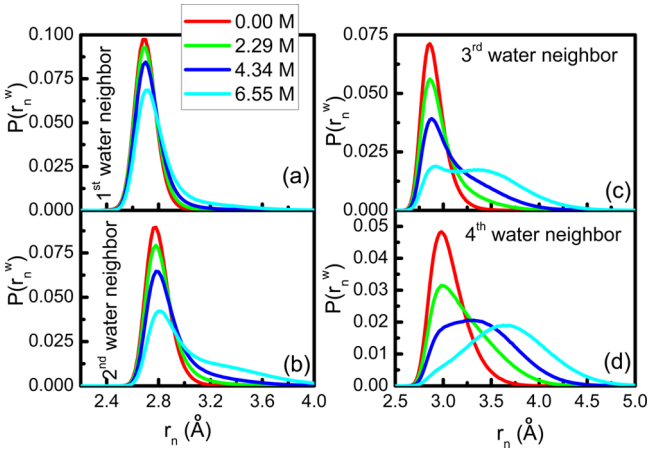

Figure 8. Distributions $P(r_n^w)$ of the distances r_n of the nth *water* neighbor from a reference water molecule for $n = 1-4$ (panels a−d).

for the first and the second neighbors do not change considerably, whereas the same for third and fourth neighbors changes considerably with increasing GdmCl concentration. This type of distortions in the radial distributions of neighbors is generally attributed to the distortion in water structure. However, if we look at these distributions carefully, at higher concentrations and for third and fourth neighbors, distributions move outward considerably beyond the average radius (around 3.5 Å) of the first solvation shell. Therefore, it is evident that at high GdmCl concentrations a significant fraction of third and fourth "water neighbors" goes out of the first solvation shell and probably other entities like Gdm^+ and Cl^- ions enter into the first solvation shell of water. [See inset of Figures 2 and 3. As GdmCl concentration increases numbers of Gdm^+ (Figure 2 inset) and Cl^- (Figure 3 inset) increase.] In the above case we considered only water molecules in choosing the first four neighbors. However, as we have found that in a concentrated GdmCl solution the probability of occupying the third and fourth neighboring positions of a central water molecule by another water molecule decreases, it is important to choose correct

DOI: 10.1021/acs.jpcb.5b03064
J. Phys. Chem. B XXXX, XXX, XXX−XXX

nearest neighbors considering all the other species also to be probable neighbors. Thus, the distortion observed in the cases of the third and fourth "water neighbors" at higher GdmCl concentrations may be arising due the water molecules that are outside the first solvation shell (generally considered to be around 3.5 Å) of water. In order to correctly choose nearest neighbors, we first chose four neighbors distance-wise, considering all the species (O_w, Gdm^+, and Cl^-) in the solution as probable neighbors, and the same distributions of radial distances are now calculated by considering only those water molecules that are within the first four neighbors. These distributions are shown in Figure 9. As expected, now we do

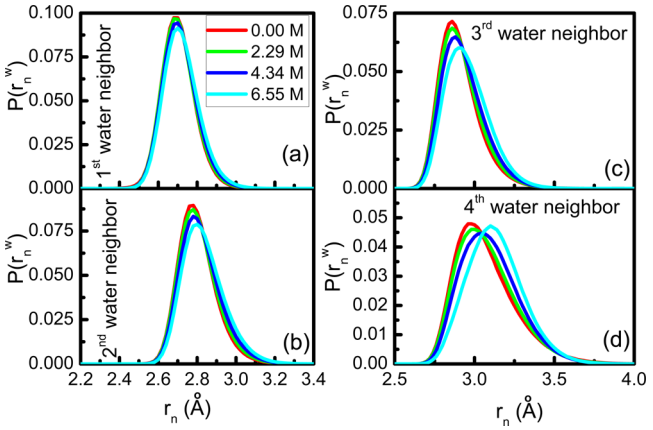

Figure 9. Same as in Figure 8, except that now, in choosing neighbors sites of Gdm^+, Cl^-, and water, all species are considered.

not find any considerable distortion in any of these distributions. Therefore, although more and more water molecules are going out of the solvation shell, radial structure of those present within the first solvation shell are not disrupted with increasing concentration of the GdmCl. In an earlier study we demonstrated the same for concentrated urea solutions.[59]

3.3.2. Tetrahedral Structure. In a perfect tetrahedral network (as in ice) a central water molecule is surrounded by its four nearest neighbors sitting at the vertices of a tetrahedron forming the first solvation shell. One usual way of measuring the tetrahedrality of a tetrahedrally coordinated fluid is to calculate average tetrahedral order parameter (cf. eq 2) and corresponding distribution. Similar quantities were used earlier[59] to gauge the tetrahedrality of urea−water solution. We calculated the average tetrahedral order parameter, $\langle q_4 \rangle$ in two different ways: by considering (i) distance-wise the first four "water neighbors" (without considering other species in solution as probable neighbors) and (ii) n ($\leq$4) water molecules which are within the (distance-wise) first four neighbors (considering Gdm^+ and Cl^- also to be probable neighbors of the central water molecule). As it is shown in Figure 10, when we consider only four "water neighbors" without considering the possibility of other species (Gdm^+, Cl^-) being the neighbors, average tetrahedral order parameter decreases significantly with increasing GdmCl concentration (see red line in Figure 10). This is understandable because, as we have shown in Figure 8, in this case many of the third and fourth "water neighbors" actually reside outside the first solvation shell. Therefore, if we consider these second-shell water molecules in our $\langle q_4 \rangle$ calculation, since they are not in the vertices (in a concentrated solution some of the vertices are occupied by other species) of the tetrahedron, the $\langle q_4 \rangle$ value will decrease. However, while choosing neighbors, if we consider that

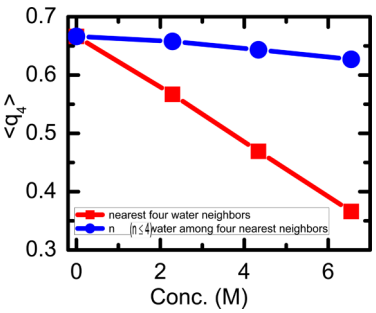

Figure 10. Average tetrahedral order parameter $\langle q_4 \rangle$ calculated by considering all the four *water* neighbors (no other species in solution is considered as a neighbor) of a reference water molecule as a function of molar concentration of GdmCl (red line with diamond symbol) and the same calculated by considering all the species (Gdm^+, Cl^- of GdmCl and O_w of water) in solution as probable neighbors and choosing only those n ($\leq$4) water molecules that are within the first four neighbors (blue line with circles).

other species such as Gdm^+ and Cl^- also as possible neighbors and choose distance-wise first four neighbors of a central water molecule, then in a concentrated GdmCl solution, all the four neighbors will not be water (as some of water neighbors are now replaced by other species). Now for calculating $\langle q_4 \rangle$, if we consider only n ($\leq$4) water neighbors that are within the first four neighbors, then the $\langle q_4 \rangle$ value does not significantly decrease with GdmCl concentration (see blue line in Figure 10). In this case, when n < 4, we have used proper normalization (see Bandyopadhyay et al.[60] for details). So, the rapid decrease in $\langle q_4 \rangle$ as a function of GdmCl concentration that was observed earlier[51] should not be attributed to breaking of tetrahedral network of water but, on the contrary, it is due to selection of wrong water neighbors. Those water molecules residing in the second shell of a central water molecule contribute to the decrease in $\langle q_4 \rangle$. Since we are using the TIP4P/2005 water model and Mandal et al.[51] used the TIP3P model in their study, we also calculated relevant structural quantities by using the TIP3P water model. The results obtained from the TIP3P model show similar trends (see Supporting Information) as those obtained from the TIP4P/2005 water model. Even when we choose correct water neighbors, a slight decrease in $\langle q_4 \rangle$ is observed (see blue line in Figure 10). Similar behavior was also observed in the case of an aqueous solution of urea.[59] The reason for this slight decrease in $\langle q_4 \rangle$ with concentration has been attributed to change in proportion of n-hydrogen-bonded molecules (with $n = 1 - 4$) in water as a function of solute concentration (see Figures 10 and 11 in the work of Bandyopadhyay et al.[59]).

3.3.3. Hydrogen-Bonding Structure. As stated in the Model and Methods section, hydrogen-bonding angle (θ_{HB}) is the angle between the line joining oxygen atoms of the two neighboring water molecules and the O−H bond of any one of the two water molecules. In order to check how first five nearest neighbors are hydrogen-bonded to the central water molecule, the distribution of θ_{HB}, $P(\theta_{HB})$ for first five "water neighbors" are shown in Figure 11. As earlier, in this case we considered only water as neighbors (without considering Gdm^+ and Cl^- ions as probable neighbors while choosing the neighbors). It is interesting to observe that the distribution does not change much for first and second neighbors, but for third and fourth neighbors (see Figure 11c,d) it changes significantly, giving rise to a new peak at around 55−60° at higher GdmCl concentration. It is interesting to observe that, for the fifth nearest neighbor, the main peak is at 55−60°. In

DOI: 10.1021/acs.jpcb.5b03064
J. Phys. Chem. B XXXX, XXX, XXX−XXX

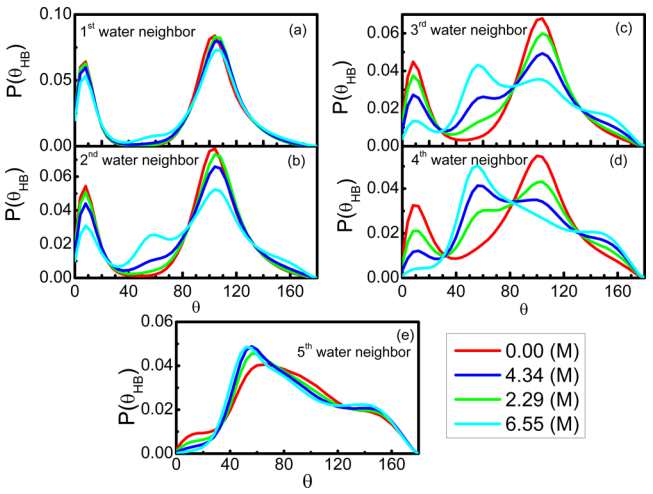

Figure 11. Distributions $P(\theta_{HB})$ of the hydrogen-bonding angle formed by a reference water molecule and one of its neighbors. Hydrogen-bonding angle θ_{HB} is the angle formed by the line joining the two oxygen atoms and the OH bond vector. In panels (a)−(e) distributions for five nearest *water* neighbors are shown. In this case, species from GdmCl molecules are not considered to be a probable neighbor.

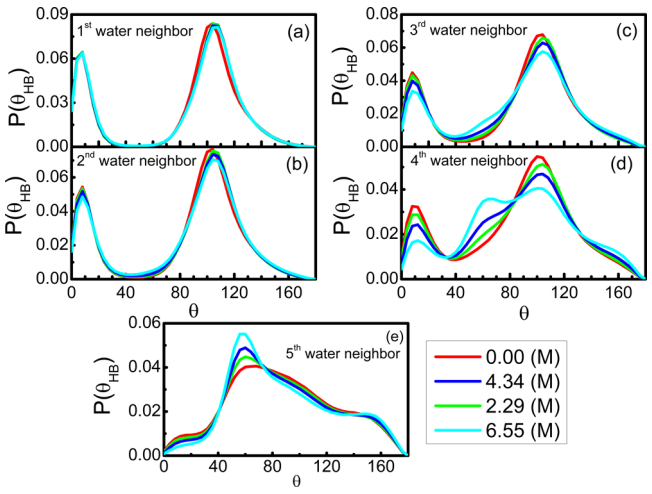

Figure 12. Same as in Figure 11, except that now we choose five nearest neighbors irrespective of whether it is any species of GdmCl or water and then calculate the required hydrogen-bonding angle between the reference water molecule and the *water* neighbor, which is within the first five (distance-wise) neighbors.

fact, we calculated (not shown here) distributions for sixth, seventh, and eighth neighboring molecules also and found that they all look like the fifth neighbor's distribution, indicating that the 55−60° peak is probably characteristic of second shell water molecules. It is also evident from the distributions of the pure water. For pure water (red curves) up to fourth nearest neighbors, there is no change in the peak positions. But for the fifth neighbor the distribution has the major peak at 55−60°. The same trend has been observed from our simulations using TIP3P water model also (see Supporting Information). However, from the HB distributions presented by Mondal et al.,[51] who used TIP3P water model, it is seen that even in pure water (with no GdmCl) the distribution of the fourth neighbor is different (in terms of positions of the peaks) from those of first, second and third neighbors and it is the same as that of the fifth neighbors (see Figure 7 in the work by Mondal et al.[51]). However, it is very unlikely; as in pure water, in the first solvation shell of water molecule there are on an average four nearest neighbors. Therefore, all first four neighbors should behave in the same way. In our simulation with TIP3P, we however observed that all the four neighbors in pure water behave in the same way and this behavior is different from that of the fifth neighboring molecule.

The emergence of 55−60° for the third and the fourth "water neighbors" (see Figure 11c,d), is probably because some of the water neighbors that we have assigned as third and fourth neighbors are actually not within the first four nearest neighbors (not within first solvation shell) if we allow other species (Gdm^+ and Cl^-) also to be probable neighbors. As we have seen in the case of the tetrahedral order parameter calculation, if we now correctly choose neighbors by considering Gdm^+ and Cl^- ions also to be probable neighbors, and consider only those water molecules that are within the first four neighbors, then the $P(\theta_{HB})$ distribution for the first three nearest neighbors are almost identical with almost no distortion (see Figure 12) with increasing GdmCl concentration. However, the distribution for the fourth neighbor still shows a small peak near 55−60° at higher GdmCl concentration. Thus, it can be concluded that fourth neighbor may not be perfectly hydrogen-bonded to the central water molecule at higher GdmCl concentrations.

In order to investigate further about the origin of the 55−60° peaks in the θ_{HB} distributions of third and fourth neighbors at higher GdmCl concentrations, we need to get idea about average relative positions of different species around a central water molecule. For that we calculated related RDFs, and those are shown in Figure 13 for two different (lowest and highest) GdmCl

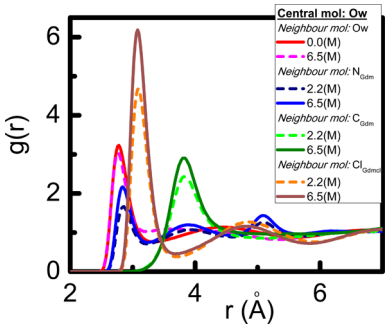

Figure 13. Radial distribution functions of O_w of water, nitrogen and carbon atoms of the guanidinium moiety and chloride ions around the O_w of water. Different color codes are described in the legend on the figure.

concentrations considered here. It is interesting to observe that carbon atom of the Gdm^+ (green curves) stays relatively far away from the central water oxygen in comparison to Cl^-, O_w of another water molecule, and nitrogen atom of Gdm^+. The O_w of water and N of Gdm^+ are almost in the same position (see red and blue sets of curves). This is because both can form HBs with the central water molecule. Chloride ions also stay in the first solvation shell of water, probably because of strong ion−dipole interaction. As far as concentration dependence is concerned, there is not much change with respect to peak position in all the cases.

As we have shown in Figure 12 that, other than O_w of neighboring water, Cl^- and nitrogen of Gdm^+ can also stay in the first solvation shell of a central water molecule, it is important to know how their presence in the first solvation shell influences the average number of water−water HBs. We therefore calculated the average number $\langle n_{HB} \rangle$ of water−water HBs as a function of

DOI: 10.1021/acs.jpcb.5b03064
J. Phys. Chem. B XXXX, XXX, XXX−XXX

GdmCl concentration. The average number of water−water HBs (see black line in Figure 14) steadily decreases with GdmCl

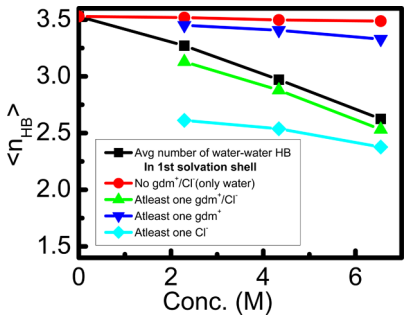

Figure 14. Average number of water−water hydrogen bonds $\langle n_{HB} \rangle$ as a function of concentration of GdmCl at different conditions (stated in the figure legend; also see the text).

concentration. Therefore, it supports the result of Figure 12, in which an additional peak (at around 55−60°) in the distribution of HB angles for the fourth nearest neighbor appeared at higher GdmCl concentration. Next, in order to get an idea about how this distortion in HB network originates, we further calculated $\langle n_{HB} \rangle$ by choosing water molecules with various restrictions. In one case, we chose all those water molecules that do not contain any Gdm^+ or Cl^- ions in their first solvation shells (i.e., all four nearest neighbors are water). In this case (see red line in Figure 14) we found negligible change in $\langle n_{HB} \rangle$ as a function of GdmCl concentration. However, if we consider only those water molecules with at least one Gdm^+ or Cl^- ions in their first solvation shell, we find (see green line) profound decrease in the average number of HB (almost the same as the black line). Now, if we choose only those water molecules with at least one Gdm^+ (no Cl^- ions) in the first solvation shell, the decrease in $\langle n_{HB} \rangle$ with GdmCl concentration (see blue line) is not so drastic (much above the average black line). However, if at least one Cl^- is present in the first solvation shell, then $\langle n_{HB} \rangle$ decreases more rapidly than the average value given by the black line. Therefore, the noticeable distortion in the HB network at high GdmCl concentrations (see Figure 12d and black line in Figure 14) arises from the presence of the Cl^- in the first solvation shell of a water molecule.

Although we have shown by calculating average number of water−water HB that the presence of Cl^- in the first solvation shell induces distortion in the water−water HB network, whether appearance of the 55−60° peak in the distribution of θ_{HB} (as shown in Figure 12d,e) is related to the presence of Cl^- in the first solvation shell is yet to be ascertained. For that purpose, we next calculated the distribution $P(\theta_{HB})$ in three different ways by imposing three different conditions, viz., considering only those water molecules that have (a) no Gdm^+/Cl^- ions in the first solvation shell (i.e., all four neighbors are water), (b) no Cl^- (but Gdm^+ and O_w can be there) in the first solvation shell, and (c) no Gdm^+ but at least one Cl^- in the first solvation shell. As shown in Figure 15a, if we choose condition (a), then the two characteristic peaks of $P(\theta_{HB})$ appear. It indicates no change in the HB network if a water molecule is surrounded by only water molecules in the first solvation shell. If we consider condition (b), then also the characteristic shape of the $P(\theta_{HB})$ distribution does not change considerably. However, if at least one Cl^- is present in the first solvation shell (condition (c)), then a new peak at around 55−60° appears in the $P(\theta_{HB})$ (see Figure 15c). Thus, it is confirmed that the new peak at 55−60° in Figure 12d is due to

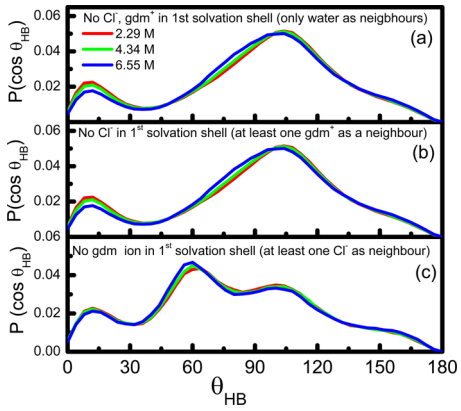

Figure 15. Distributions $P(\theta_{HB})$ of the hydrogen-bonding angle calculated by imposing three different conditions (see figure legend and also see the text).

the presence of Cl^- in the first solvation shell of water. It is to be noted that this 55−60° peak in the $P(\theta_{HB})$ distribution can also appear if a water molecule chosen as a neighbor is actually in the second solvation shell of the central water molecule.

3.4. Effect of Guanidinium Chloride Concentration on Dynamical Properties. Translational diffusivities D of the different species in solution can be calculated from the respective mean-squared displacement (MSD) values using the Einstein relation, viz.,

$$D = \frac{1}{2d}\lim_{t\to\infty}\frac{\langle \Delta r^2 \rangle}{\Delta t} = \frac{1}{2d}\lim_{t\to\infty}\frac{\langle |\mathbf{r}(t) - \mathbf{r}(0)|^2 \rangle}{\Delta t} \quad (5)$$

where $\langle \Delta r^2 \rangle$ is the MSD averaged over number of particles and time origins. In the above equation, $\mathbf{r}(t)$ is the position vector at time t and d is the dimensionality of the system. The MSDs of water, Gdm^+, and Cl^- at three different concentrations are displayed in Figure S6 of the Supporting Information. The MSD decreases with increasing concentration of GdmCl for all the species including water in the solution. The diffusivity values calculated from the slope of the MSD plots at different concentrations for the three different species are shown in Table 2.

Table 2. Diffusivity Values for Water, Gdm^+, and Cl^- at Different GdmCl Concentrations

system	concn (M)	D(water) ($\times 10^{-5}$ cm^2/s)	$D(Gdm^+)$ ($\times 10^{-5}$ cm^2/s)	$D(Cl^-)$ ($\times 10^{-5}$ cm^2/s)
1G	0.00	2.040 ± 0.147		
2G	2.29	1.259 ± 0.035	0.396 ± 0.158	0.595 ± 0.065
3G	4.34	0.683 ± 0.019	0.202 ± 0.007	0.370 ± 0.044
4G-1	6.55	0.257 ± 0.002	0.046 ± 0.010	0.087 ± 0.001

The pure water diffusion coefficient is calculated to be 2.04 × 10^{-5} cm^2/s and a similar value has been obtained earlier.[61] Diffusivity values for all the species decrease considerably with increasing GdmCl concentration (see Table 2).

3.5. An Arginine-Rich Peptide in the Aqueous Solution of Guanidinium Chloride. As already mentioned the aggregation of Gdm^+ and its parallel stacking can have implications in the mechanism of unfolding of an ARG-rich protein or peptide. The ARG side chain of a protein or peptide has a similar moiety as Gdm^+ (see the C1 carbon along with N2, N9, and N10 of ARG in Figure 1B). Therefore, there is a possibility that the Gdm^+ moiety will attack the similar moiety of

DOI: 10.1021/acs.jpcb.5b03064
J. Phys. Chem. B XXXX, XXX, XXX−XXX

ARG and in this case also Gdm^+ will be stacked in parallel to the ARG moiety. As already stated, in order to check this hypothesis, we simulated an ARG-rich peptide (PDB ID: 2MIA) in a 6 M GdmCl solution. We show the results for ARG−Gdm^+ and Gdm^+−Gdm^+ RDFs as obtained from the peptide simulation in Figure 16. In the same figure, we also show the Gdm^+−Gdm^+

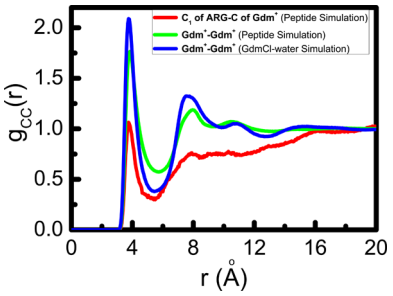

Figure 16. Radial distribution functions of the carbon atom of the Gdm^+ moiety of GdmCl around the C1 carbon atom (see Figure 1B) of the ARG side chain of the protein (red line) in protein−GdmCl−water system, carbon atom of the Gdm^+ moiety of GdmCl around the same of other GdmCl molecule in the protein−GdmCl−water system (green line), and carbon atom of the Gdm^+ moiety of GdmCl around the same of other GdmCl molecules in the GdmCl−water (without protein) system (blue line).

RDF obtained from aqueous solution of GdmCl (without peptide). The first peak of the $g(r)$ in all these three cases is in the same position, indicating the ARG−Gdm^+ pair is forming aggregates similar to the Gdm^+−Gdm^+ aggregates in aqueous salt solution. In the peptide solution, the first peak of ARG−Gdm^+ RDF is smaller than that of Gdm^+−Gdm^+ RDF, indicating that Gdm^+ ions in the peptide solution are in the close vicinity of only the exposed ARG sites of the peptide. This fact is further supported by the depletion region beyond the first solvation shell seen (see red curve in Figure 16) in the ARG−Gdm^+ RDF of the peptide solution. Similar phenomena have been observed in the case of a small tetra-arginine peptide.[26]

The guanidinium moiety formed by the N2, C1, N9 and N10 atoms of the ARG is separated by three carbon atoms (C3, C4, and C5; see Figure 1B) from the α carbon of the peptide main chain. In order to further pinpoint that the Gdm^+ moiety of the GdmCl salt comes close to the guanidinium moiety (C1 atom) of the ARG, we have further calculated the RDFs of Gdm^+ around different carbon atoms (C1, C3, C4, and C5 atoms) of the ARG side chain and are shown in Figure 17. As expected, the Gdm^+ of the salt comes closer to the C1 carbon atom of ARG as compared to other carbon center of ARG. The peak height in this case (around C1 atom) is also larger than that corresponding to other carbon centers. Thus, it clearly indicates that Gdm^+ attacks the guanidinium moiety (C1 carbon center) of the ARG.

In order to further investigate the possibility of parallel stacking between the Gdm^+ and ARG moieties, we calculated the probability distribution of the angle made by the Gdm^+ plane and the ARG plane (where ARG plane is defined by the C1−N2−N9−N10 (see Figure 1A) atom centers of ARG side chain). The calculated probability distributions for ARG−ARG and Gdm^+−Gdm^+ planes as obtained from the peptide simulation are shown in Figure 18. In both the cases parallel orientations are observed. Thus, it is demonstrated that the Gdm^+ moiety of the Gdm^+ not only attacks the guanidinium moiety of the ARG side chain, but also forms a parallel stacking configuration with the same.

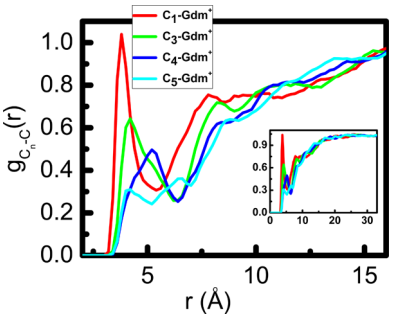

Figure 17. Radial distribution functions of the carbon atom of the Gdm^+ moiety of GdmCl around the C1 carbon atom of the ARG side chain (red line), C3 carbon atom of the ARG side chain of the protein (green line), C4 carbon atom of the ARG side chain of the protein (blue line), and C5 carbon atom of the ARG side chain of the protein (cyan line) in the protein−GdmCl−water system (see Figure 1B for ARG ball-and-stick model). In the inset, same plots with longer range are shown.

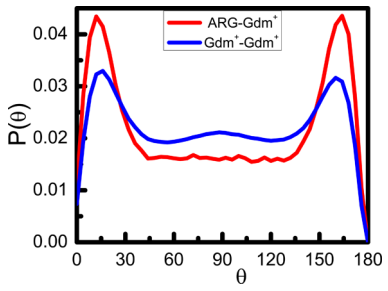

Figure 18. Distributions $P(\theta)$ of the angles θ made by the perpendiculars drawn from the molecular plane formed by carbon and three nitrogen atoms of Gdm^+ moiety in the GdmCl and the molecular plane of the guanidinium moiety formed by C1, N2, N9, and N10 atoms of the ARG side chain of the protein (see Figure 1B).

4. SUMMARY AND CONCLUSIONS

In order to elucidate the effects of GdmCl concentration on the extent of like-charge Gdm^+−Gdm^+ ion-pair formation and on the local structure of water, we have performed molecular dynamics simulations of aqueous GdmCl solutions of different concentrations ranging from 0 to 6.50 M. Analyses of the carbon−carbon (of Gdm moiety) radial distribution functions reveal the like-charge ion-pairing with a clear existence of contact-pair and solvent-separated states. It has been stated[22,24] that the driving force behind this type of like-charge ion-pair formation is the collapse of weakly hydrated planar Gdm^+ moieties. As the concentration of GdmCl increases, although the height of the first peak decreases and that of the second peak of $g_{CC}(r)$ increases, the actual numbers of Gdm^+ ions in both the contact-pair and solvent-separated states increase. Since the individual $g_{CC}(r)$ profile is normalized with respect to the bulk concentration, the peak height in RDF actually signifies the relative density of the species at the peak position as compared to the bulk (away from the center) density. Thus, although peak heights of $g_{CC}(r)$ decrease with increasing concentration, the absolute number of Gdm^+ ions in both the contact and solvent-separated states increases with increasing concentration of the GdmCl solution (see inset of Figure 1). The position of the first peak in the $g_{CC}(r)$ (see Figure 2) at 3.7 Å excludes side-wise association and indicates possible parallel stacking of the Gdm^+ moieties. Indeed, the appearance of two peaks at around 0° and 180° in the distribution of angles between two Gdm planes (as

DOI: 10.1021/acs.jpcb.5b03064
J. Phys. Chem. B XXXX, XXX, XXX−XXX

shown in Figure 5) corroborates parallel stacking of the Gdm^+ moieties.

The existence of such like-charge ion-pair stacking in GdmCl aqueous solution has two implications. As GdmCl at sufficiently high concentration denatures proteins, the like-charge ion-pair formation indicates the tendency of the Gdm^+ moieties to stack against the structurally similar ARG moieties in proteins. In order to test this hypothesis, we simulated an ARG-rich peptide in an aqueous solution of 6 M GdmCl. The results clearly demonstrate that Gdm^+ ions stack against the ARG side chain of the peptide. In fact, Gdm^+ attacks the guanidinium moiety of the ARG, and it is also shown that the stacking is in parallel orientation. Thus, it supports a direct mechanism of chemical denaturation of a protein by GdmCl. In fact, many other studies[45−54] have advocated a direct preferential interaction mechanism of protein denaturation by GdmCl. On the other hand, the like-charge ion association in aqueous solution also signifies that, due to this affinity, during protein folding ARG and other similar moieties will come close to each other. In fact, from the structural analyses of proteins it has been observed that ARG and other similar group stack together, and the orientation of the guanidinium group of ARG is parallel to the side chains of aromatic amino acid residues.[14,71,72] The temperature dependence of the distribution of orientation angles between two Gdm^+ molecular planes shows decreasing orientational preferences with increasing temperature, consistent with the temperature-induced denaturation of proteins.

As already stated, apart from the direct mechanism, an indirect effect of breaking water structure by the GdmCl at higher concentrations has also been suggested by many researchers.[27−44] The results presented herein highlight the effect of the presence of GdmCl at higher concentrations on the radial, tetrahedral, and hydrogen-bonding structures of water. It is shown that, if nearest neighbors are chosen properly by allowing Gdm^+ and Cl^- ions also to be possible neighbors (other than water molecules) of a central water molecule, then radial and tetrahedral structures remain intact, even at GdmCl concentration as high as 6.55 M. In an earlier study, we demonstrated the same for an aqueous solution of urea as well.[59] However, in the case of a hydrogen-bonding structure, it is surprising to notice that, at high enough GdmCl concentration, the distributions of hydrogen-bonding angles made by the third and fourth neighbors to the central molecules get distorted. Also the average number of hydrogen bonds decreases steadily with increasing concentration. But in the case of another denaturant, urea, it was shown[59] that the hydrogen-bonding structure of water was not broken even at a concentration as high as 9 M. Further analyses show (Figures 14 and 15) that the decrease in average number of hydrogen bonds and the uncharacteristic peak at $\theta_{HB} = 55−60°$ in the distribution of θ_{HB} (as seen in Figure 12) arise due to presence of Cl^- in the solvation shell of the water.

■ ASSOCIATED CONTENT

Supporting Information

Part A, important results using TIP3P water model; Part B, results for system size dependence and different simulation times; Part C, mean-squared displacements of different species in GdmCl−water system. The Supporting Information is available free of charge on the ACS Publications website at DOI: 10.1021/acs.jpcb.5b03064.

■ AUTHOR INFORMATION

Corresponding Author

*E-mail: nihcho@barc.gov.in, niharc2002@yahoo.com, or niharc2007@gmail.com. Tel.: +91-22-2559 5089. Fax: +91-22-2551 5151.

Notes

The authors declare no competing financial interest.

■ ACKNOWLEDGMENTS

We thank Dr. B. N. Jagatap, Bhabha Atomic Research Centre (BARC), Mumbai, India, for his support and encouragement. Thanks are also due to Computer Division, BARC, for providing ANUPAM supercomputing facility and support.

■ REFERENCES

(1) Nozaki, Y.; Tanford, C. The Solubility of Amino Acids and Related Compounds in Aqueous Urea Solutions. *J. Biol. Chem.* **1963**, *238*, 4074−4081.

(2) Tanford, C. Contribution of Hydrophobic Interactions to the Stability of the Globular Conformation of Proteins. *J. Am. Chem. Soc.* **1962**, *84*, 4240−4247.

(3) Brandts, J. F.; Hunt, L. Thermodynamics of Protein Denaturation. III. Denaturation of Ribonuclease in Water and in Aqueous Urea and Aqueous Ethanol Mixtures. *J. Am. Chem. Soc.* **1967**, *89*, 4826−4838.

(4) Yancey, P. H.; Clark, M. E.; Hand, S. C.; Bowlus, R. D.; Somero, G. N. Living with Water Stress: Evolution of Osmolyte Systems. *Science* **1982**, *217*, 1214−1222.

(5) Alonso, D. O. V.; Dill, K. A. Solvent Denaturation and Stabilization of Globular Proteins. *Biochemistry* **1991**, *30*, 5974−5985.

(6) Watlaufer, D. B.; Malik, S. K.; Stoller, L.; Coffin, R. L. Nonpolar Group Participation in the Denaturation of Proteins by Urea and Guanidinium Salts. Model Compound Studies. *J. Am. Chem. Soc.* **1964**, *86*, 508−514.

(7) Tanford, C.; Kawahara, K.; Lapanje, S. Proteins in 6 M Guanidine Hydrochloride. Demonstration of Random Coil Behaviour. *J. Biol. Chem.* **1966**, *241*, 1921−1923.

(8) Hammes, G. G.; Schimmel, P. R. An Investigation of Water−Urea and Water−Urea−Polyethylene Glycol Interactions. *J. Am. Chem. Soc.* **1967**, *89*, 442−446.

(9) Tanford, C.; Aune, K. C. Thermodynamics of the Denaturation of Lysozyme by Guanidine hydrochloride. III. Dependence on Temperature. *Biochemistry* **1970**, *9*, 206−211.

(10) Greene, R. F.; Pace, C. N. Urea and Guanidine Hydrochloride Denaturation of Ribonuclease, Lysozyme, α-chymotrypsin, and β-lactoglobulin. *J. Biol. Chem.* **1974**, *249*, 5388−5394.

(11) Pfeil, W.; Privalov, P. L. Thermodynamic Investigations of Proteins. II. Calorimetric Study of Lysozyme Denaturation by Guanidine Hydrochloride. *Biophys. Chem.* **1976**, *4*, 33−40.

(12) Makhatadze, G. I.; Privalov, P. L. Protein Interactions with Urea and Guanidinium Chloride. A Calorimetric Study. *J. Mol. Biol.* **1992**, *226*, 491−505.

(13) Bennion, B. J.; Daggett, V. The Molecular Basis for the Chemical Denaturation of Proteins by Urea. *Proc. Natl. Acad. Sci. U. S. A.* **2003**, *100*, 5142−5147.

(14) Tsumoto, K.; Umetsu, M.; Kumagai, I.; Ejima, D.; Philo, J. S.; Arakawa, T. Role of Arginine in Protein Refolding, Solubilization, and Purification. *Biotechnol. Prog.* **2004**, *20*, 1301−1308.

(15) Arakawa, T.; Tsumoto, K. The effects of Arginine on Refolding of Aggregated Proteins: Not Facilitate Refolding, but Suppress Aggregation. *Biochem. Biophys. Res. Commun.* **2003**, *304*, 148−152.

(16) Reddy, R. C.; Lilie, K. H.; Rudolph, R.; Lange, C. L-Arginine Increases the Solubility of Unfolded Species of Hen Egg White Lysozyme. *Protein Sci.* **2005**, *14*, 929−935.

(17) Pednekar, D.; Tendulkar, A.; Durani, S. Electrostatics-Defying Interaction between Arginine Termini as a Thermodynamic Driving Force in Protein-Protein Interaction. *Proteins: Struct., Funct., Genet.* **2009**, *74*, 155−163.

DOI: 10.1021/acs.jpcb.5b03064
J. Phys. Chem. B XXXX, XXX, XXX−XXX

(18) Hirano, A.; Kameda, T.; Arakawa, T.; Shiraki, K. Arginine-Assisted Solubilization System for Drug Substances: Solubility Experiment and Simulation. *J. Phys. Chem. B* **2010**, *114*, 13455−13462.
(19) Arakawa, T.; Ejima, D.; Tsumoto, K.; Obeyama, N.; Tanaka, Y.; Kita, Y.; Timasheff, S. N. Suppression of Protein Interactions by Arginine: A Proposed Mechanism of the Arginine Effects. *Biophys. Chem.* **2007**, *127*, 1−8.
(20) Bogan, A. A.; Thorn, K. S. Anatomy of Hot Spots in Protein Interfaces. *J. Mol. Biol.* **1998**, *280*, 1−9.
(21) Boudon, S.; Wipff, G.; Maigret, B. Monte Carlo Simulations on the Like-Charged Guanidinium-Guanidinium Ion Pair in Water. *J. Phys. Chem.* **1990**, *94*, 6056−6061.
(22) Vazdar, M.; Vymetal, J.; Heyda, J.; Vondrasek, J.; Jungwirth, P. Like-Charge Guanidinium Pairing from Molecular Dynamics and Ab-initio Calculations. *J. Phys. Chem. A* **2011**, *115*, 11193−11201.
(23) Soetens, J. C.; Millot, C.; Chipot, C.; Jansen, G.; Ángyán, J. G.; Maigret, B. Effect of Polarizability on the Potential of Mean Force of Two Cations. The Guanidinium−Guanidinium Ion Pair in Water. *J. Phys. Chem. B* **1997**, *101*, 10910−10917.
(24) Vazdar, M.; Uhlig, F.; Jungwirth, P. Like-Charge Ion Pairing in Water: An Ab Initio Molecular Dynamics Study of Aqueous Guanidinium Cations. *J. Phys. Chem. Lett.* **2012**, *3*, 2021−2024.
(25) Shih, O.; England, A. H.; Dallinger, G. C.; Smith, J. W.; Duffey, K. C.; Cohen, R. C.; Prendergast, D.; Saykally, R. J. Cation-Cation Contact Pairing in Water: Guanidinium. *J. Chem. Phys.* **2013**, *139*, 035104-1−035104-7.
(26) Kubickova, A.; Krizek, T.; Coufal, P.; Wernersson, E.; Heyda, J.; Jungwirth, P. Guanidinium Cations Pair with Positively Charged Arginine Side Chains in Water. *J. Phys. Chem. Lett.* **2011**, *2*, 1387−1389.
(27) Wernersson, E.; Heyda, J.; Vazdar, M.; Lund, M.; Mason, P. E.; Jungwirth, P. Orientational Dependence of the Affinity of Guanidinium Ions to the Water Surface. *J. Phys. Chem. B* **2011**, *115*, 12521−12526.
(28) Caballero-Herrera, A.; Nordstrand, K.; Berndt, K. D.; Nilsson, L. Effect of Urea on Peptide Conformation in Water: Molecular Dynamics and Experimental Characterization. *Biophys. J.* **2005**, *89*, 842−857.
(29) Schellman, J. A. Selective Binding and Solvent Denaturation. *Biopolymers* **1987**, *26*, 549−559.
(30) Muller, N. A Model for the Partial Reversal of Hydrophobic Hydration by Addition of a Urea-like Cosolvent. *J. Phys. Chem.* **1990**, *94*, 3856−3859.
(31) Wallqvist, A.; Covell, D. G.; Thirumalai, D. Hydrophobic Interactions in Aqueous Urea Solutions with Implications for the Mechanism of Protein Denaturation. *J. Am. Chem. Soc.* **1998**, *120*, 427−428.
(32) Shortle, D.; Chan, H. S.; Dill, K. A. Modeling the Effects of Mutations on the Denatured States of Proteins. *Protein Sci.* **1992**, *1*, 201−215.
(33) Ohtaki, H.; Radnai, T. Structure and Dynamics of Hydrated Ions. *Chem. Rev.* **1993**, *93*, 1157−1204.
(34) Soper, A. K.; Luzar, A. Orientation of Water Molecules around Small Polar and Nonpolar Groups in Solution: A Neutron Diffraction and Computer Simulation Study. *J. Phys. Chem.* **1996**, *100*, 1357−1367.
(35) Vanzi, F.; Madan, B.; Sharp, K. Effect of the Protein Denaturants Urea and Guanidinium on Water Structure: A Structural and Thermodynamic Study. *J. Am. Chem. Soc.* **1998**, *120*, 10748−10753.
(36) Shimizu, A.; Fumino, K.; Yukiyasu, K.; Taniguchi, Y. NMR Studies on Dynamic Behavior of Water Molecule in Aqueous Denaturant Solutions at 25° C: Effects of Guanidine Hydrochloride, Urea and Alkylated Ureas. *J. Mol. Liq.* **2000**, *85*, 269−278.
(37) Chitra, R.; Smith, P. E. Molecular Association in Solution: A Kirkwood−Buff Analysis of Sodium Chloride, Ammonium Sulfate, Guanidinium Chloride, Urea, and 2,2,2-Trifluoroethanol in Water. *J. Phys. Chem. B* **2002**, *106*, 1491−1500.
(38) Canchi, D. R.; Paschek, D.; García, A. E. Equilibrium Study of Protein Denaturation by Urea. *J. Am. Chem. Soc.* **2010**, *132*, 2338−2344.
(39) England, J. L.; Haran, G. Role of Solvation Effects in Protein Denaturation: From Thermodynamics to Single Molecules and Back. *Annu. Rev. Phys. Chem.* **2011**, *62*, 257−277.
(40) Klimov, D. K.; Straub, J. E.; Thirumalai, D. Aqueous Urea Solution Destabilizes Aβ16−22 Oligomers. *Proc. Natl. Acad. Sci. U. S. A.* **2004**, *101*, 14760−14765.
(41) Akhtar, Md. S.; Ahmad, A.; Bhakuni, V. Guanidinium Chloride- and Urea-Induced Unfolding of the Dimeric Enzyme Glucose Oxidase. *Biochemistry* **2002**, *41*, 3819−3827.
(42) Frank, H. S.; Franks, F. Structural Approach to the Solvent Power of Water for Hydrocarbons; Urea as a Structure Breaker. *J. Chem. Phys.* **1968**, *48*, 4746−4757.
(43) Franks, F. In *Water: A Comprehensive Treatise*; Plenum: New York, 1973; Vol. *2*, pp 1−54.
(44) Soper, A. K.; Castner, E. W.; Luzar, A. Impact of Urea on Water Structure: A Clue to Its Properties as a Denaturant? *Biophys. Chem.* **2003**, *105*, 649−666.
(45) Kuharski, R. A.; Rossky, P. J. Solvation of Hydrophobic Species in Aqueous Urea Solution: A Molecular Dynamics Study. *J. Am. Chem. Soc.* **1984**, *106*, 5794−5800.
(46) Kuharski, R. A.; Rossky, P. J. Molecular Dynamics Study of Solvation in a Urea-Water Solution. *J. Am. Chem. Soc.* **1984**, *106*, 5786−5793.
(47) Godawat, R.; Jamadagni, S. N.; Garde, S. Unfolding of Hydrophobic Polymers in Guanidinium Chloride Solutions. *J. Phys. Chem. B* **2010**, *114*, 2246−2254.
(48) Ma, L.; Pegram, L.; Record, M. T.; Cui, Q. Preferential Interactions between Small Solutes and the Protein Backbone: A Computational Analysis. *Biochemistry* **2010**, *49*, 1954−1962.
(49) Batchelor, J. D.; Olteanu, A.; Tripathy, A.; Pielak, G. J. Impact of Protein Denaturants and Stabilizers on Water Structure. *J. Am. Chem. Soc.* **2004**, *126*, 1958−1961.
(50) Wei, H.; Fan, Y.; Gao, Y. Q. Effects of Urea, Tetramethyl Urea, and Trimethylamine N-Oxide on Aqueous Solution Structure and Solvation of Protein Backbones: A Molecular Dynamics Simulation Study. *J. Phys. Chem. B* **2010**, *114*, 557−568.
(51) Mandal, M.; Mukhopadhyay, C. Concentration-Dependent Like-Charge Pairing of Guanidinium Ions and Effect of Guanidinium Chloride on the Structure and Dynamics of Water from All-Atom Molecular Dynamics Simulation. *Phys. Rev. E* **2013**, *88*, 052708-1−052708-10.
(52) Idrissi, A.; Gerard, M.; Damay, P.; Kiselev, M.; Puhovsky, Y.; Cinar, E.; Lagant, P.; Vergoten, G. The Effect of Urea on the Structure of Water: A Molecular Dynamics Simulation. *J. Phys. Chem. B* **2010**, *114*, 4731−4738.
(53) Stumpe, M. C.; Grubmüller, H. Urea Impedes the Hydrophobic Collapse of Partially Unfolded Proteins. *Biophys. J.* **2009**, *96*, 3744−3752.
(54) Lim, W. K.; Rosgen, J.; Englander, S. W. Urea but Not Guanidinium, Destabilizes Proteins by Forming Hydrogen Bonds to the Peptide Group. *Proc. Natl. Acad. Sci. U. S. A.* **2009**, *106*, 2595−2600.
(55) Choudhury, N.; Pettitt, B. M. On the Mechanism of Hydrophobic Association of Nanoscopic Solutes. *J. Am. Chem. Soc.* **2005**, *127*, 3556−3567.
(56) Choudhury, N. On the Manifestation of Hydrophobicity at the Nanoscale. *J. Phys. Chem. B* **2008**, *112*, 6296−6300.
(57) Mason, P. E.; Neilson, G. W.; Dempsey, C. E.; Barnes, A. C.; Cruickshank, J. M. The Hydration Structure of Guanidinium and Thiocyanate Ions: Implications for Protein Stability in Aqueous Solution. *Proc. Natl. Acad. Sci. U. S. A.* **2003**, *100*, 4557−4561.
(58) Mason, P. E.; Neilson, G. W.; Enderby, J. E.; Saboungi, M. L.; Dempsey, C. E.; MacKerell, A. D.; Brady, J. W. The Structure of Aqueous Guanidinium Chloride Solutions. *J. Am. Chem. Soc.* **2004**, *126*, 11462−11470.
(59) Bandyopadhyay, D.; Mohan, S.; Ghosh, S. K.; Choudhury, N. Molecular Dynamics Simulation of Aqueous Urea Solution: Is Urea a Structure Breaker? *J. Phys. Chem. B* **2014**, *118*, 11757−11768.
(60) Bandyopadhyay, D.; Mohan, S.; Ghosh, S. K.; Choudhury, N. Correlation of Structural Order, Anomalous Density, and Hydrogen Bonding Network of Liquid Water. *J. Phys. Chem. B* **2013**, *117*, 8831−8843.

DOI: 10.1021/acs.jpcb.5b03064
J. Phys. Chem. B XXXX, XXX, XXX−XXX

(61) Abascal, J. L. F.; Vega, C. A General Purpose Model for the Condensed Phases of Water: TIP4P/2005. *J. Chem. Phys.* **2005**, *123*, 234505-1−234505-12.
(62) Casu, F.; Duggan, B. M.; Hennig, M. The Arginine-Rich RNA-Binding Motif of HIV-1 Rev is Intrinsically Disordered and Folds upon RRE Binding. *Biophys. J.* **2013**, *105*, 1004−1017.
(63) Van Der Spoel, D.; Lindahl, E.; Hess, B.; Groenhof, G.; Mark, A. E.; Berendsen, H. J. C. GROMACS: Fast, Flexible, and Free. *J. Comput. Chem.* **2005**, *26*, 1701−1718.
(64) Allen, M. P.; Tildesley, D. J. *Computer Simulation of Liquids*; Oxford University Press: New York, 1987.
(65) Parrinello, M.; Rahman, A. Polymorphic Transitions in Single Crystals: A New Molecular Dynamics Method. *J. Appl. Phys.* **1981**, *52*, 7182−7190.
(66) Berendsen, H. J. C.; Postma, J. P. M.; van Gunsteren, W. F.; DiNola, A.; Haak, J. R. Molecular Dynamics with Coupling to an External Bath. *J. Chem. Phys.* **1984**, *81*, 3684−3690.
(67) Hess, B.; Bekker, H.; Berendsen, H. J. C.; Fraaije, J. G. E. M. LINCS: A Linear Constraint Solver for Molecular Simulations. *J. Comput. Chem.* **1997**, *18*, 1463−1472.
(68) Darden, T.; York, D.; Pedersen, L. Particle Mesh Ewald: An N log(N) Method for Ewald Sums in Large Systems. *J. Chem. Phys.* **1993**, *98*, 10089−10092.
(69) Essmann, U.; Perera, L.; Berkowitz, M. L.; Darden, T.; Lee, H.; Pedersen, L. G. A Smooth Particle Mesh Ewald Potential. *J. Chem. Phys.* **1995**, *103*, 8577−8592.
(70) Errington, J. R.; Debenedetti, P. G. Relationship between Structural Order and the Anomalies of Liquid Water. *Nature* **2001**, *409*, 318−321.
(71) Flocco, M. M.; Mowbray, S. L. Planar Stacking Interactions of Arginine and Aromatic Side-Chains in Proteins. *J. Mol. Biol.* **1994**, *235*, 709−717.
(72) Mitchell, J. B. O.; Nandi, C. L.; McDonald, I. K.; Thornton, J. M.; Price, S. L. Amino/Aromatic Interactions in Proteins: Is the Evidence Stacked against Hydrogen Bonding? *J. Mol. Biol.* **1994**, *239*, 315−331.

DOI: 10.1021/acs.jpcb.5b03064
J. Phys. Chem. B XXXX, XXX, XXX−XXX